

Advanced Uses of Weather Radar into Analysis and Prediction of Rainfall for Hydrological Applications

Eiichi Nakakita

Associate Prof., Dept. of Global Environment Engineering, Kyoto University, Kyoto, Japan

Yoshiharu Suzuki

Graduate Student, Dept. of Global Environment Engineering, Kyoto University, Kyoto, Japan

Shuichi Ikebuchi

Prof., Disaster Prevention Research Institute, Kyoto University, Kyoto, Japan

ABSTRACT: As one of advanced uses of radar, a physically based rainfall prediction method which uses a conceptual rainfall model assimilated by information from volume scanning radar is shown. As another example of advanced utilization of weather radar, results from analyzing a hierarchical time-scale structure in dependency of rainfall distribution on topography are shown.

1 INTRODUCTION

1.1 Short-term Rainfall Prediction

Rainfall distribution is greatly affected by topography. That is, dynamics and microphysics relate topography to features such as generation, growth, decay and lingering of rainfall areas. This is why, so far, no short-term rainfall prediction method using weather radar has been successful in predicting rainfall distribution on meso- β scale beyond approximately two hours ahead. This situation is severe in Japan because 70 percent of its land area is mountainous. Improving short-term rainfall prediction is necessary in order to increase the reliability of real-time flood forecasting. In this sense, utilizing radar information into prediction with meteorological basic equations is to be expected to improve above situation. Many methods of short-term rainfall prediction using weather radar have been proposed in Japan and in other countries. Nakakita et al. (1996) and Browning and Collier (1989) review other methods including methods that use satellite measurements.

Short-term rainfall prediction methods can be classified into three categories; (1) methods based on the linear extrapolation of the movement pattern of horizontal rainfall distribution, (2) methods based on a conceptual rainfall model using the principles of water balance and thermodynamics; and (3) meso-scale numerical weather forecasting models. Most of the current short-term rainfall prediction methods that use radar information belong to the first category. It is apparent, however, that the temporal variation of the rainfall distribution is excessively complicated to be expressed by such simple extrapolation methods, especially over mountainous regions. The method belonging to (1) can practically be used until only one-hour prediction lead-time. On the other hand, current operational numerical prediction works well beyond the lead-time of twelve hours. However, it is the fact that the accuracy of prediction for lead-times of two to twelve hours is quite low. In order to improve the accuracy in these lead-times, physically based prediction methods assimilated with radar information is required. In this sense, development of methods belonging to (2) and (3) has been expected to improve the accuracy.

A method belonging to the second category has developed by Nakakita et al., 1990, 1991, 1992, 1996 and this is operationally used by the River Bureau of Ministry of Land, Infrastructure and Transportation, Japan. Kalman filtering theory was also introduced to this method for more practical use (Sugimoto, Nakakita and Ikebuchi, 2000). Also, Georgakakos and Bras (1984a, b) and Lee and Georgakakos (1990) have been developing their own conceptual models, introducing stochastic concepts such as Kalman filtering theory into their models. On the other hand, Japan Meteorological Agency started forecast service based on meso-scale numerical model.

Our main concern has been developing a conceptual model that can express effects of topography on rainfall distribution. We proposed that a water balance concept should be introduced physically into short-term rainfall prediction. We also suggested that the use of a volume scanning radar is indispensable to realize this.

1.2 Analysis of Rainfall Distribution over Mountainous Region

As mentioned above, it is very difficult to determine the properties of rainfall distribution in Japan, which is a mountainous region, due to the influence of topography. Additionally, due to physical restrictions, it is not possible to set up rain gauges at a large number of locations in such regions. As a result, rainfall distribution structures in mountainous regions are not yet obvious.

One of the common features of conventional studies is that the accumulation time scale of rainfall that is analyzed is relatively short scale, that is, the time scale of one or two rainfall events. Oki et al. (1990), for example, explained well the concept of the relation between topographic effect on accumulated rainfall distribution and its temporal-spatial scale, and reached the following conclusion. In the case that the accumulation time scale is a little longer than the temporal-spatial scale of an individual meteorological disturbance, that is to say, in the time scale of one rainfall event or daily rainfall, the topographic effect becomes very significant. The above conclusion is agreed with in this study. However if the rainfall distribution in such an accumulation time scale is paid attention to, it seems to be difficult to determine the properties of rainfall distribution as the topographic effect on rainfall varies significantly with each meteorological disturbance.

On the other hand, Nakakita et al., 1997 suggested the following. It may be possible to find a universal relation between rainfall and topography independently of the variation of rainfall with each disturbance, if the topographic effect over an even longer accumulation time scale is paid special attention to. That is to say, it is necessary to take such a long time scale into consideration that covers the scale of plural meteorological disturbances for the purpose of determining the universal properties of rainfall distribution.

In conventional studies the data obtained from ground-based rain gauges that are set at discrete locations are used as true rainfall data. However there seems to exist a limit of reproducibility of rainfall distribution in mountainous regions if it is analyzed by using such data, which doesn't have adequate observation density in mountainous regions.

In this study one of the properties of rainfall distribution, that is, a hierarchical time-scale structure in the dependence of rainfall distribution on topography is paid special attention to. It is attempted to determine the universal properties of the dependence on topography, and to make clear rainfall distribution structure through the analysis of rainfall data observed by weather radars.

2 SHORT-TERM RAINFALL PREDICTION USING CONCEPTUAL RAINFALL MODEL AND VOLUME SCANNING RADAR

2.1 Outline of the Short-term Prediction Method

As a basic environmental meso- α scale field, distributions of air pressure, wind velocity, air temperature and water vapor are estimated using the grid point values from a numerical weather prediction. Grid point values (for three hourly intervals) from a numerical weather prediction are generated by the Regional Spectral Model developed by the Japan Meteorological Agency and are known as Grid Point Value data (GPV data). The estimated wind field is kept unchanged throughout the prediction process. At the initial time, three-dimensional distributions of water content and rainfall intensity, as meso- β scale information, are estimated from radar observations. Also the initial three-dimensional distribution of the conversion rate of water vapor is estimated as meso- β scale information using already estimated distributions. Next, based on these distributions, three-dimensional distribution of parameter of the conceptual rainfall model is identified as meso- β scale information. After horizontally translating the above estimated parameter's distribution, three-dimensional distributions of the conversion rate and then the rainfall intensity are predicted. The reason for the simple translation of the parameter's distribution is that we strive for, by parameter's distribution of a conceptual rainfall model, modeling a field not affected by topography.

It should be noted that the method does not use the predicted GPV rainfall itself. The horizontal and temporal resolutions of the GPV data are still low compared to those of radar information. Thus, the additional radar information allows the GPV subgrid variability of rainfall to be predicted. This subgrid variability is crucial to accurate flood forecasting during extreme events in mountainous topography. The physically-based model utilizes observations of a volume scanning radar as information on meso- β scale and predictions of a numerical weather model as a meso- α scale information. The model parameter can be taken as a kind of index which shows degree of shortages of vertical vapor flux estimated by using basic meso- α wind field. Thus, the conceptual rainfall model plays the role of bridging the gap between radar information and numerical weather prediction scales.

prediction scales.

Specifically, the following three conservation equations are used:

$$\frac{\partial \theta}{\partial t} + u \frac{\partial \theta}{\partial x} + v \frac{\partial \theta}{\partial y} + w \frac{\partial \theta}{\partial z} = \frac{LQ}{\rho} \left(\frac{1000}{p} \right)^{R_d / C_p}, \quad (1)$$

$$\frac{\partial m_v}{\partial t} + u \frac{\partial m_v}{\partial x} + v \frac{\partial m_v}{\partial y} + w \frac{\partial m_v}{\partial z} = -\frac{Q}{\rho}, \quad (2)$$

$$\frac{\partial m_l}{\partial t} + u \frac{\partial m_l}{\partial x} + v \frac{\partial m_l}{\partial y} + w \frac{\partial m_l}{\partial z} = \frac{Q}{\rho} + \frac{\rho_w}{\rho} \frac{\partial r}{\partial z}, \quad (3)$$

while the following equation for estimating the rainfall intensity is adopted only for prediction stage:

$$r = \frac{\rho}{\rho_w} W_t m_l, \quad (4)$$

It should be noted that (1)-(4) are used in both conceptual rainfall models. In (1)-(4), (x, y, z) represents the Cartesian coordinate system, (u, v, w) is the wind vector, θ is the potential temperature, m_l and m_v are the mixing ratios of the liquid water content and water vapor respectively, r is the rainfall intensity, Q is the water vapor conversion rate, ρ and ρ_w are densities of the air and liquid water respectively, L is the latent heat of condensation, C_p is the specific heat at constant pressure, R_d is the individual gas constant for dry air, and p is the air pressure in hPa. W_t is the averaged relative fall velocity of water particles computed by the empirical equations of *Ogura and Takahashi* [1971].

The most important variable in (1)-(4) is the water vapor conversion rate Q because its prediction will in turn affect the predictions of other variables including rainfall intensity r . The "conversion rate" is defined as the amount of water vapor that is converted into precipitation particles per unit time and unit volume. The initial three-dimensional distribution of Q is estimated using the distributions of m_l and r based on the conservation equation (3). The conceptual rainfall model then predicts the time series of the distribution of Q , which results in rainfall prediction. It should be noted that there is no provision for prediction of clouds because conventional radars cannot detect cloud particles.

The Instability Field, IF, model is defined by the following equation:

$$\frac{\partial}{\partial t} \{(1-\delta)m_s\} + u \frac{\partial}{\partial x} \{(1-\delta)m_s\} + v \frac{\partial}{\partial y} \{(1-\delta)m_s\} + w \frac{\partial}{\partial z} \{(1-\delta)m_s\} = -\frac{Q}{\rho} \quad (5)$$

where, m_s is the saturation mixing ratio computed using the following empirical formula given by *Murray* [1967] and *Pielke* [1984]

$$m_s = \frac{3.8}{p} \exp \left\{ \frac{T(\theta, p) - 273.2}{T(\theta, p) - 35.9} \right\} \quad (6)$$

In (6) the expression of the air temperature $T(\theta, p)$ means that T can be computed following the definition of potential temperature θ and the air pressure p .

With the radar estimated conversion rate Q we can then compute the initial three-dimensional distribution of $\delta(x, y, z)$ from (5) when Q is not zero. Here, the three-dimensional distribution of the parameter δ defines the instability field of the IF model. The relation $1-\delta = mv/ms$ is found to hold only after δ is identified. Using the past and present three-dimensional distributions of radar reflectivity, past and present instability fields can be identified.

Equation (5) assumes water vapor beyond a newly defined saturation mixing ratio, $(1-\delta)m_s$, condenses to the precipitation particles (or precipitation particles evaporate when water vapor mixing ratio is less than

($1-\delta$)ms). In other words, domains with large values of parameter δ are prone to relatively heavy rainfall. Therefore, the parameter δ can be taken as a kind of index which shows the degree of shortages of vertical water vapor flux brought on by the used basic meso- α wind field. The reason for the shortages is that the used wind field, corresponding to the meso- α scale, is rather stratiform; this is in contrast with organized strong convection accompanied by the moisture, which is expected to exist in the cumulative clouds in the scale of meso- β .

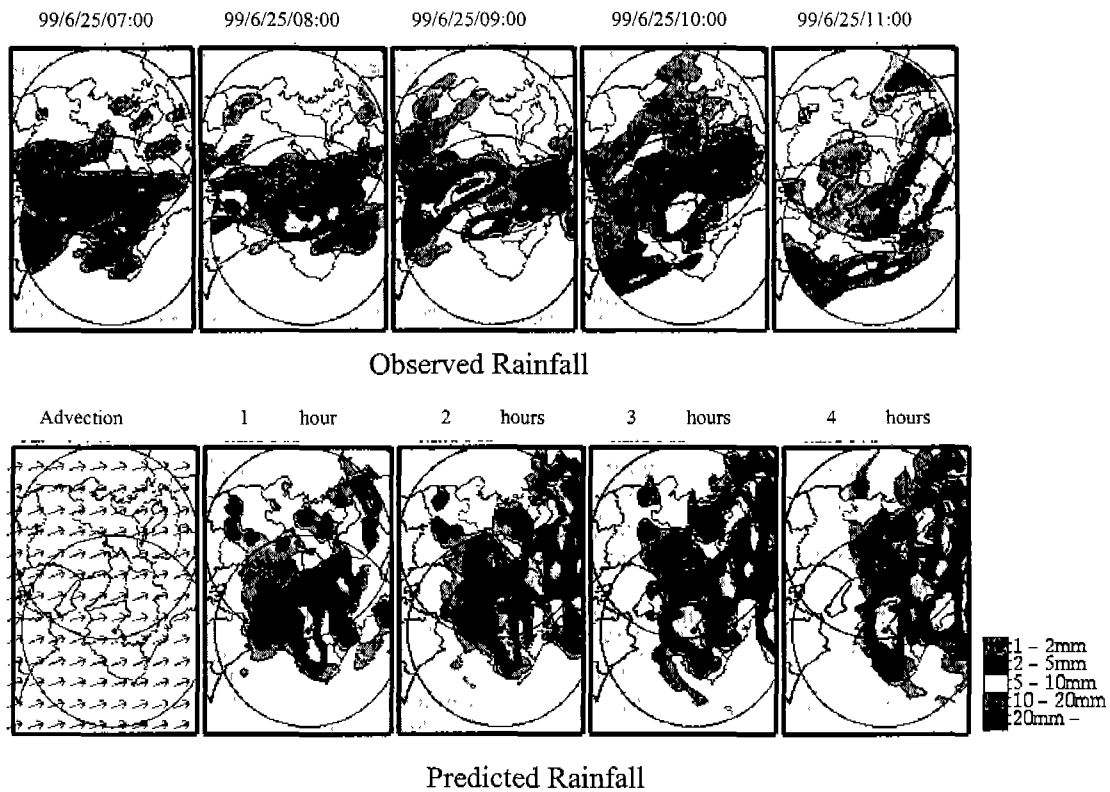


Fig.1 Rainfall distribution predicted using conceptual rainfall model assimilated by 3D radar information.

2.2 Case Study

Fig.1 shows radar-observed and predicted rainfall distributions for hourly intervals. The translation vector is identified using time series of horizontal rainfall distributions for the past 30 minutes according to the operationally used method proposed by Takasao and Shiiba (1985). The upper line shows the radar-observed distributions and the right column shows predicted distributions both for the height of 3.5km. The starting time of prediction is 07:00 JST, June 25 in 1999.

It can be seen that gradual expansion of hole rainfall area and local growth of rainfall area over southern mountainous region are well predicted. These kind of predictions have not been possible with liner extrapolation of radar echo pattern.

3 HIERARCHICAL TIME-SCALE STRUCTURE IN THE DEPENDENCE OF RAINFALL DISTRIBUTION ON TOPOGRAPHY

3.1 Hierarchical Time-scale Structure of Rainfall Distribution

Spatial rainfall distributions at accumulation time scales of between 5 and 25 days are shown in Fig.3. Here, radius of the target domain is 120 km and the resolutions of radar information are three km in space and

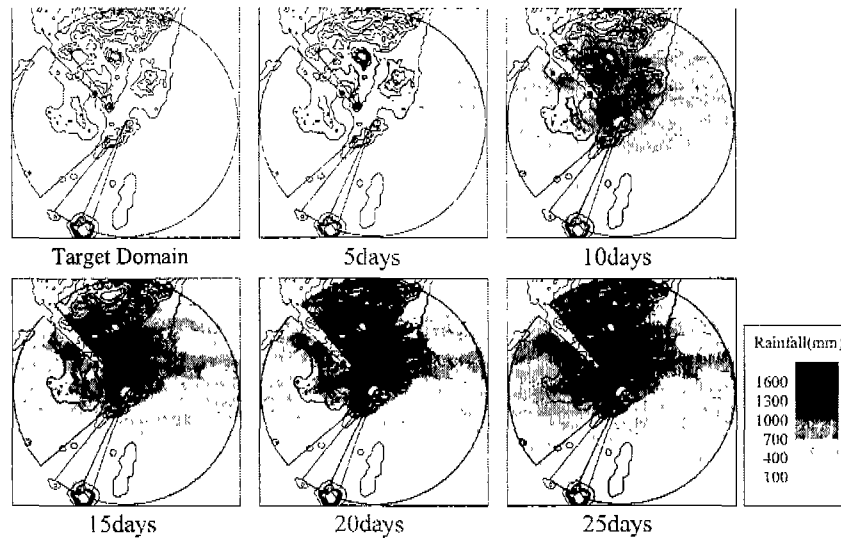


Fig. 2 Accumulated rainfall distributions at various time scales. (southern Kyushu region, from August 1, 1993)

five minutes in time. In this figure it is shown that the relation between rainfall distribution and topographic altitude becomes obvious as the accumulation time scale of rainfall increases. Additionally it is shown that the relation doesn't vary so significantly in the accumulation time scale longer than approximately 20 days, and appears to converge into a constant relation as the time scale increases.

The correlation coefficient (C.C) between T -days-accumulated rainfall distribution for each point, $R_T(x,y)$, and topographic altitude, $h(x,y)$, is then calculated while changing the accumulation time scale. The results are presented in Fig.3. This figure also demonstrates that the correlation coefficient increases as the accumulation time scale increases, and that after the time scale reaches approximately a month the value becomes almost constant.

These properties of rainfall distribution demonstrate the following. Although the relation between short time-scale rainfall distribution (ex. one-event rainfall distribution) and topography varies in a number of ways, predominant topographic effects and the universal relations can be found only if the relation between relatively long time-scale rainfall distribution (ex. one-week or one-month rainfall distribution) and topography is taken into consideration. This concept is represented in a schematic form in Fig.4.

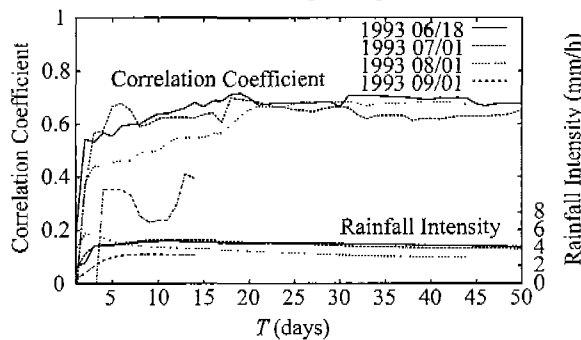


Fig. 3 Correlation coefficient between T -days-accumulated rainfall $R_T(x,y)$ and topographic altitude $h(x,y)$. (southern Kyushu region)

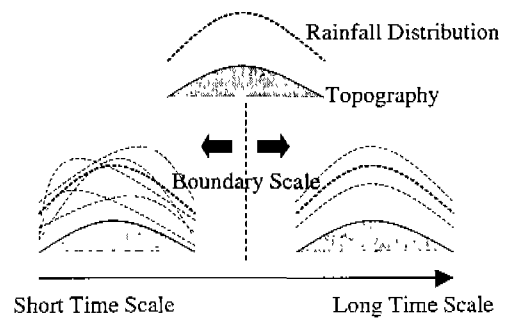


Fig. 4 Schematic figure of the hierarchical time-scale structure of rainfall distribution.

In this study this feature of rainfall distribution is called "hierarchical time-scale structure in the dependence of rainfall distribution on topography". Drawing attention to this, an attempt is made to quantify the dependence of rainfall distribution on topography, which has been difficult in conventional studies. That is to say an attempt is made to determine rainfall distribution structures in various time scales, including short and long time scales. In this paper the analysis of the hierarchical time-scale structure that is being attempted will be

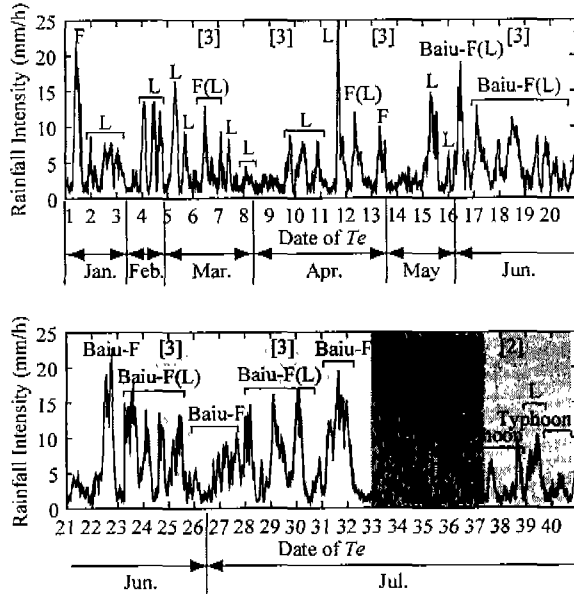


Fig. 5 Imaginary time series of regional average rainfall intensity. (southern Kyushu region, 1993)

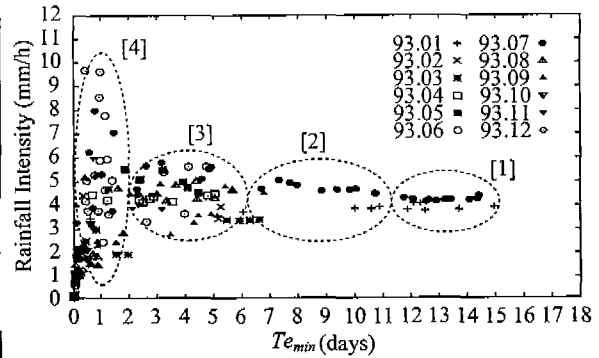


Fig. 6 The smallest time scale Te_{min} and regional average rainfall intensity.

presented.

3.2 Boundary Scales of the Hierarchical Time-scale

3.2.1 The Relations Between Boundary Scales and Types of Rainfall Events

It is necessary to know the time scales which are the boundary of the hierarchical structure so as to make clear its properties. That is to say, it is important to determine if it is a universal feature of rainfall that the boundary scale is approximately 20 days as shown in Fig.3 and 4. Therefore researches have been conducted to determine the smallest accumulation time scale Te_{min} at which the correlation coefficient between rainfall distribution and topographic altitude become high enough. However if there is a long period with no rain or with only a little rain in a accumulation period, the smallest time scale Te_{min} is influenced and increases. It is necessary to remove the influence by excluding such a dry period for the purpose of the analysis of the time scale Te_{min} . Therefore imaginary time series of rainfall intensity was created only with the data of which regional average is over 1 mm/h, and is used to research the smallest time scale Te_{min} changing the start time of accumulation on the imaginary time series.

By the way, so as to exclude a dry period without breaking the continuity of rainfall in a duration of rainfall, the value of regional average rainfall intensity of 1 mm/h is chosen as a limit value. Excluding a dry period also provides the advantage that ground clutters in a dry period can be removed. This imaginary time series of rainfall intensity is represented in Fig.5. In this study the time scale on the imaginary time series is called effective rainfall time (E.R.T.) and is expressed as Te (days). At the same time, the smallest time scale Te_{min} on the imaginary time series is expressed as Te_{min} (days).

The smallest time scale Te_{min} at which the correlation coefficient between Te -days-average rainfall distribution $R_{Te}(x,y)$ and topographic altitude $h(x,y)$ becomes over 0.73 is calculated for the imaginary time series. The result is represented in Fig.6. In this figure the marks of plots are expressed as the month of the start time of accumulation. In this analysis however, rainfall distribution and topographic altitude were smoothed by using the moving average method (averages of an approximately 21 km square grid are used) so as to make the hierarchical time-scale structure clearer. As a result, the correlation coefficient increased by approximately 0.1 on the whole. The correlation coefficient value of 0.73 was chosen as the most suitable value to make the boundary time scale of the hierarchical structure clearer. Fig.6 shows that the smallest time scale Te_{min} varies from less than 1 day to around 15 days.

The plots in Fig.6 are then classified into 4 cases according to the time scale of the horizontal axis, and the case numbers are labeled. In Fig.5 the case numbers are also labeled according to the start time of accumulation of each case. The types of rainfall events on a large scale that is estimated with weather maps are shown in Fig.5. In the figure L is expressed as a low pressure system, F is expressed as a frontal system and F(L) is expressed as a low pressure system with a front.

These figures show that Case-[1], where the time scale Te_{min} is the longest, corresponds to the case where accumulation of rainfall began during the period with Baiu rainfall in July. Case-[2], where the time scale Te_{min} is the second longest, corresponds to the case where accumulation of rainfall began during the period with a series

of typhoons in late July. In the same way, it is shown that Case-[3] corresponds to the period with low pressure systems. As a result, it is demonstrated that the properties of the relation between rainfall distribution and topographic altitude on a large scale vary greatly according to the types of rainfall events (ex. rainfall with a low pressure system or a frontal system).

Additionally, the various types of rainfall events on a small scale, for example stratiform rainfall or convective rainfall, are taken into account in the following section.

3.2.2 Spatial Distribution of the Length of a Rainfall Period and Boundary Scales of the Hierarchical Structure

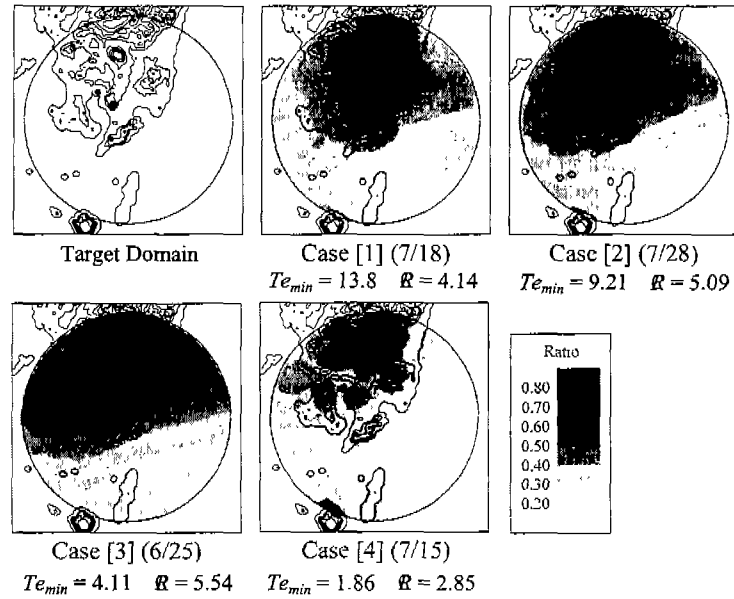


Fig. 7 The length of a rainfall period where rainfall over 1 mm/h is observed at each point, which is expressed as the ratio toward Te_{min} (days). (R : regional average rainfall intensity (mm/h), southern Kyushu region, 1993)

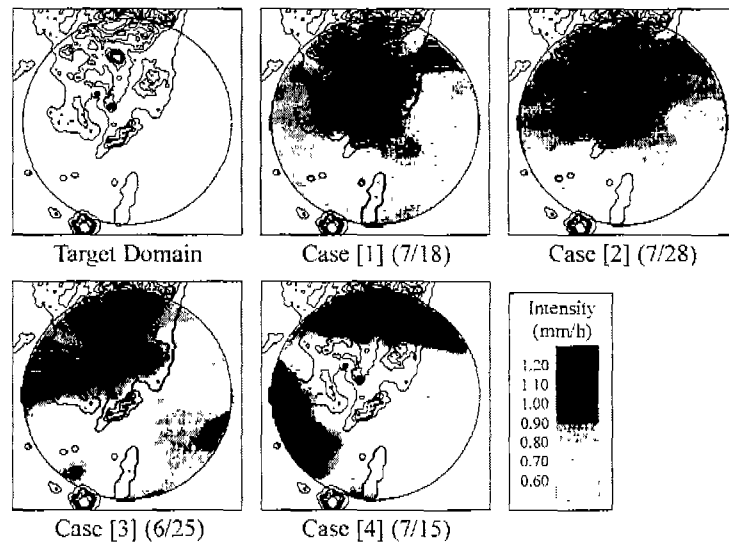


Fig. 8 The distribution of rainfall intensity where rainfall over 1 mm/h is observed at each point. (southern Kyushu region, 1993)

It is considered that there are two factors that determine the dependence of rainfall distribution on topography. One is the dependence of rainfall intensity, and the other is the dependence of the length of a rainfall period. Therefore it is necessary to distinguish the two factors when the effect on rainfall distributions of topography is considered.

First, the length of a rainfall period where a rainfall over 1 mm/h is observed at each point in the target domain is calculated to determine which is the main factor of the variation of the time scale Te_{min} according to the types of rainfall events. The results are represented in Fig.7. Each figure in Fig.7 corresponds to an example from each case displayed in Fig.6. They are expressed as the ratio between the length of a rainfall period, where rainfall over 1 mm/h is observed, and the smallest time scale Te_{min} .

These figures demonstrate the following. In Case-[1] corresponding to the case of rainfall with frontal systems, where the time scale Te_{min} is the longest, the value of the ratio is relatively small on the whole, and the spatial bias toward mountainous regions of the value is also small. Case-[2] corresponding to the case of rainfall with typhoons appears to have a larger bias toward mountainous regions than Case-[1], and Case-[3] which had rainfall with low pressure systems appears to have an even larger bias than Case-[2]. That is to say, as the time scale Te_{min} becomes smaller, the bias toward mountainous regions becomes larger. For Case-[4], where the time scale Te_{min} is the smallest, its relation to the types of rainfall events is not apparent. It is, however, considered that the time scale Te_{min} is the smallest since a rainfall greatly depending on topography occurred by accident.

Generally speaking, a rainfall with a frontal system includes both a small region with a convective rainfall and a large region with a stratiform rainfall. Thus it can be said that Case-[1] corresponds to the case of a stratiform rainfall. On the other hand, Case-[2] and Case-[3] can be said to correspond to the case of a convective rainfall, which is under little influence of atmospheric conditions on the synoptic scale differently from a stratiform rainfall. Therefore Fig.7 shows that the accumulation time scale, which was necessary until the topographic effect became predominant, is longer in the case of a stratiform rainfall than in the case of a convective rainfall.

Additionally in the case of a stratiform rainfall, the dependence of the length of a rainfall period on topography is considered to be relatively small, since the rainfall frequency is influenced by an atmospheric condition on the synoptic scale. In the case of a convective rainfall, the dependence is considered to be large, since the frequency of generation of convective cells is significantly influenced by topography, which can become a trigger for generating an ascending air current. The results shown in Fig.7 are consistent in these respects.

Second, the following is confirmed in terms of the dependence of rainfall intensity on topography. The distribution of average rainfall intensity during the period where a rainfall over 0.1 mm/h is observed at each point is calculated. The results in Fig.8 shows the following. The dependence of rainfall intensity doesn't differ so greatly with the types of rainfall events. Additionally the degree of dependence on topography is smaller than that of the rainfall frequency. The dependence of rainfall intensity in the case of a convective rainfall is a little larger than in the case of a stratiform rainfall.

As the result of the above consideration, the following conclusions are obtained. In the case of a convective rainfall, the rainfall frequency greatly depends on topography, and thus the dependence of the rainfall intensity on topography can be said to be relatively small. The great dependence of the rainfall frequency is the main reason that the correlation coefficient between rainfall distribution and topography becomes high enough to be over 0.73 in a relatively short accumulation time scale. In the case of a stratiform rainfall, the rainfall frequency and the rainfall intensity depend on topography to almost the same extent. They are, however, quite smaller than the dependence of the rainfall frequency in the case of a convective rainfall. Therefore it is necessary to accumulate the dependences of them for a long period until topographic effects become apparent. In other words, the difference of the dependence of the rainfall frequency is the main reason that the smallest time scale Te_{min} differs greatly with the type of the rainfall event, that is, depending on whether it is a convective rainfall or a stratiform rainfall.

As described above, it is considered necessary to take the types of rainfall events into account so as to determine the hierarchical time-scale structure of rainfall distribution in detail in the future. Therefore a method to distinguish the types of rainfall events by using three-dimensional information from weather radars is to be created, and utilized for the analysis of the hierarchical time-scale structure of rainfall.

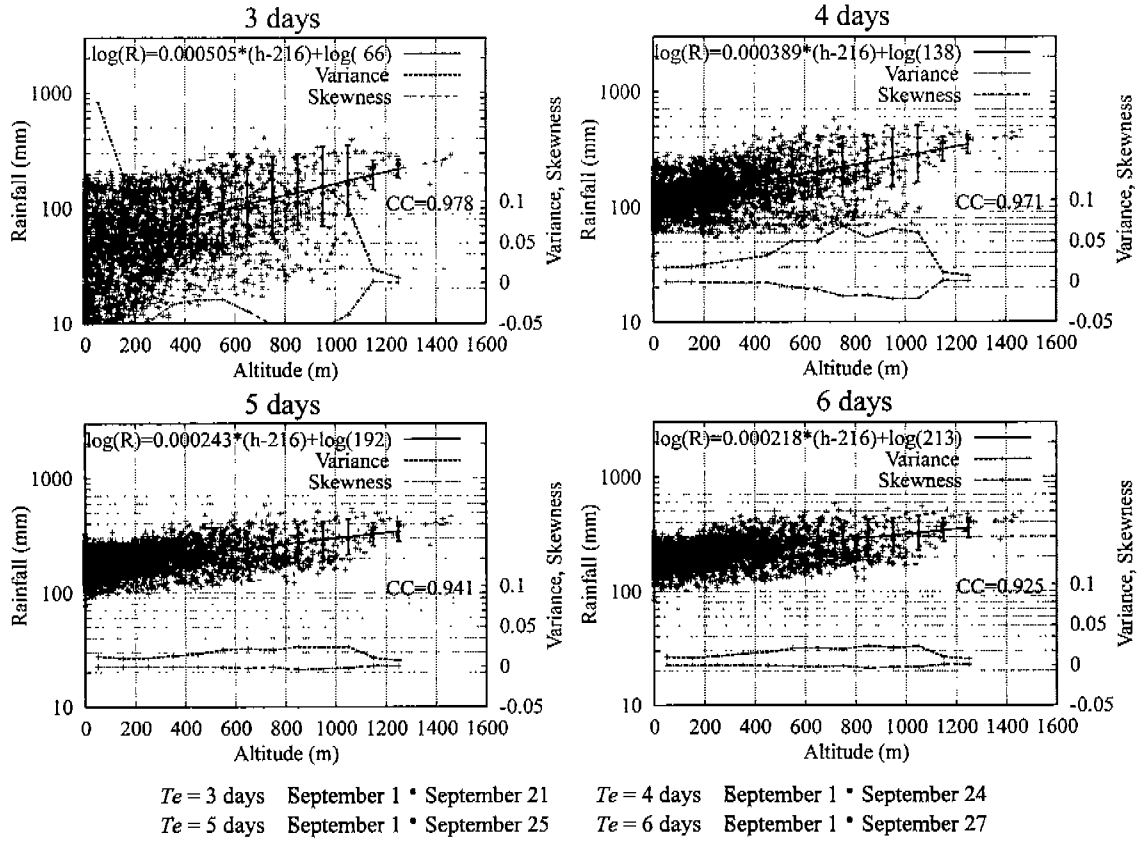


Fig. 9 Accumulated rainfall and topographic altitude at each accumulation time scale T_e . (Kinki region, from September 1, 1998)

3.3 Indices for the Expression of the Hierarchical Time-scale structure

3.3.1 Properties of Rainfall Distribution in the Kinki Region of Japan

In this section the properties of rainfall distribution in the Kinki region of Japan is investigated. For the effective rainfall time T_e , 0.3 mm/h is chosen as a threshold value. This investigation shows that the relation between rainfall distribution and topographic altitude becomes apparent as the accumulation time T_e increases, as is the same feature of rainfall distribution in the southern Kyushu (Fig.2). Such a tendency is so outstanding around the Kii Mountains, which is based in the south of the Kinki region. However, unlike the southern Kyushu region, there exit some regions where the dependence of rainfall on topography is not apparent, for example coastal regions of the Sea of Japan.

The correlation coefficient between T_e -days-accumulated rainfall distribution and topographic altitude is calculated, as it was for Fig.3. When compared to the result in Fig.3, features different from those of the southern Kyushu region are found, that is, the correlation coefficient doesn't increase with rainfall accumulation and doesn't tend to converge into a constant value. As a result, it is necessary to use another index besides correlation coefficient so as to analyze the hierarchical time-scale structure of rainfall distribution in the Kinki region. In the following section another index is introduced.

3.3.2 Analysis of the Hierarchical Structure through Classification of Topographic Altitude

The figures displayed in Fig.90 represent the relation between topographic altitude, on the horizontal axis, and T_e -days-accumulated rainfall, on the vertical axis. In these figures all points in the target domain are plotted. Each figure represents a case with accumulation time scales T_e of between 3 days and 6 days. In every case it is

shown that accumulated rainfall tends to increase on the whole with the increase of topographic altitude. Although such a qualitative tendency has already been reported in conventional studies which used ground-based rain-gauge data, it remains one of the challenges to formulate such properties of rainfall distribution.

Here, the topographic altitude is classified at 100 m intervals, and then a regression line is made by using the special averages of accumulated rainfall for each class. The results are shown in Fig.9. These results demonstrate that it may be possible to determine the dependence of rainfall distribution on topography, since the correlation coefficient between the special averages of accumulated rainfall and topographic altitude for each class indicates a high value, which is over 0.9. Additionally in each class, the variance and skewness of accumulated rainfall on a logarithmic axis, $\log(R)$, from the regression line are calculated. The results are also shown in Fig.9. These results show that the variance of accumulated rainfall in each class decreases with the increase of accumulation time, and converges into a constant value. That is to say, the relation between rainfall distribution and topographic altitude converges into a constant relation as rainfall accumulation time increases. This is the feature of hierarchical time-scale structure of rainfall distribution.

Even in these cases, the variance decreases as the accumulation time scale T_e increases, and then converges into an almost constant value after the T_e increases to be over about 5 days. This feature indicates the existence of a hierarchical time-scale structure and that 5 days of T_e is one of the boundary time scales. Additionally the slope of the regression line also converges into an almost constant value at the point of about 5 days of T_e . As described above, the slope of the regression line converges into an almost constant value, and the variance also converges into a constant value. That is to say, it is demonstrated that the dependence of rainfall distribution on topography can be quantified by using such statistic values as an index only if rainfall distribution of which accumulation time is over a certain value, since the regression line represents a expected value of accumulated rainfall distribution and forms the basis of this analysis.

4 REFERENCES

- Browning, K. A. and C. G. Collier, Nowcasting of precipitation systems, *Review of Geophysics*, 27 No.3, 658-664, 1989.
- Georgakakos, K. P. and R. L. Bras, A hydrologically useful station precipitation model, Part I: Formulation, *Water Resour. Res.*, 20, No.11, 1585-1596, 1984a.
- Georgakakos, K. P. and R. L. Bras, A hydrologically useful station precipitation model, Part II: Applications, *Water Resour. Res.*, 20, No.11, 1597-1610, 1984b.
- Lee, T. H. and K. P. Georgakakos, A two-dimensional stochastic-dynamical quantitative precipitation forecasting model, *J. Geophys. Res.*, 95-D3, 2113-2126, 1990.
- Nakakita, E., T. Sugahara, N. Okada, and S. Ikebuchi : Temporal-spatial rainfall distribution characteristics depending on topographical features (in Japanese with English abstract), *Annals of the Disaster Prevention Research Institute of Kyoto University*, No.40 B-2, pp.275-287, 1997.
- Rahuel, J.L., Holly, F.M., Jr., Chollet, J.P., Belleudy, P.J., and Yang, G. (1989). "Modeling of river bed evolution for bedload sediment mixtures." *J. Hydr. Engrg.*, ASCE, Vol. 115, No. 11, pp. 1521-1542.
- Nakakita, E., M. Shiiba, S. Ikebuchi, and T. Takasao, Advanced use into rainfall prediction of three-dimensionally scanning radar, *Hydrological applications of weather radar*, edited by I. C. Clukie and C. G. Collier, 391-408, 1991.
- Nakakita, E., S. Ikebuchi, N. Sawada, M. Shiiba and T. Takasao, A short-term rainfall prediction method using reflectivity detected by three-dimensionally scanning radar, *Preprints of 2nd Int. Symp. on Hydrological Applications of Weather Radar*, F1, Hannover, Germany, 10pages, 1992.
- Nakakita, E., S. Ikebuchi, T. Nakamura, M. Kanmuri, M. Okuda and A. Yamaji, Short-term rainfall prediction method using a volume scanning radar and grid point value data from numerical weather prediction, *J. Geophys. Res.*, 101-D21, 26,181-26-197, 1996.
- Nakakita, E., S. Ikebuchi, N. Sawada, M. Shiiba and T. Takasao, A short-term prediction method using reflectivity detected by three-dimensionally scanning radar, *Advanced in Hydrological Applications of Weather Radar*, Proc. of the 2nd Int. Symp. on Hydrological Applications of Weather Radar, Hannover, Germany, 1998.
- Oki, T., K. Mushiake, and T. Koike : Rainfall distribution at storm event estimated by orography and wind direction (in Japanese with English abstract), *Journal of the Japan Society of Civil Engineers*, Vol.417 II-13, pp.199-207, 1990.
- Sugimoto, S., E. Nakakita, S. Ikebuchi, A stochastic approach to short-term rainfall prediction using a physically based conceptual rainfall model, *J. Hydrol.*, 242, 137-155, 2001.